JPET Fast Forward. Published on November 2, 2016 as DOI: 10.1124/jpet.116.236984
This article has not been copyedited and formatted. The final version may differ from this version.

JPET #236984

Role of Equilibrative Nucleobase Transporter 1/SLC43A3 as a Ganciclovir Transporter in the Induction of Cytotoxic Effect of Ganciclovir in a Suicide Gene Therapy with Herpes Simplex Virus Thymidine Kinase

Junji Furukawa, Katsuhisa Inoue, Kinya Ohta, Tomoya Yasujima, Yoshihisa Mimura, and Hiroaki Yuasa

Department of Biopharmaceutics, Graduate School of Pharmaceutical Sciences, Nagoya City University, Nagoya, Japan (J.F., T.Y., Y.M., H.Y.), College of Pharmacy, Kinjo Gakuin University, Nagoya, Japan (K.O.), and Department of Biopharmaceutics, School of Pharmacy, Tokyo University of Pharmacy and Life Sciences, Tokyo, Japan (K.I.)

JPET #236984

Running Title: Role of ENBT1 as a GCV Transporter in HSV-TK/GCV Therapy

Corresponding author: Katsuhisa Inoue, Ph.D.

Department of Biopharmaceutics, School of Pharmacy, Tokyo University of Pharmacy and Life Sciences

1432-1 Horinouchi, Hachioji, Tokyo 192-0392, Japan

Tel: 042-676-3126

Fax: 042-676-3126

E-mail: kinoue@toyaku.ac.jp

Number of text pages: 33

Number of tables: 0

Number of figures: 11

Number of references: 22

Number of words in Abstract: 249

Number of words in Introduction: 614

Number of words in Discussion: 1025

ABBREVIATIONS: ANOVA, analysis of variance; ENBT1, equilibrative nucleobase transporter 1; ENT, equilibrative nucleoside transporter; GCV, ganciclovir; GFP, green fluorescent protein; HEK293, human embryonic kidney 293; MDCKII, Madin-Darby canine kidney II; HSV-TK, herpes simplex virus thymidine kinase; IC_{50}, half inhibition concentration; K_m, Michaelis constant; PCR, polymerase chain reaction; RT, reverse transcription; V_{max}, maximum transport rate.

Recommended section assignment: Metabolism, Transport, and Pharmacogenomics

ABSTRACT

A suicide gene therapy using herpes simplex virus thymidine kinase (HSV-TK) with ganciclovir (GCV) has been under development as a tumor-targeted therapy. However, the mechanism of cellular GCV uptake, which is prerequisite in the therapy, has not been clarified. In an attempt to resolve this situation and gain information to optimize HSV-TK/GCV system for cancer therapy, we found that human equilibrative nucleobase transporter 1 (ENBT1) can transport GCV with a Michaelis constant of 2.75 mM in Madin-Darby canine kidney II (MDCKII) cells stably transfected with this transporter. In subsequent experiments using green fluorescent protein (GFP)-tagged ENBT1 (GFP-ENBT1) and HSV-TK, the uptake of GCV (30 μM), which was minimal in MDCKII cells and unchanged by their transfection with HSV-TK alone, was found to be increased extensively by their transfection with GFP-ENBT1 together with HSV-TK. Accordingly, cytotoxicity, which was assessed by the WST-8 cell viability assay after the treatment of those cells with GCV (30 μM) for 72 h, was induced in those transfected with GFP-ENBT1 together with HSV-TK but not in those transfected with HSV-TK alone. These results suggest that ENBT1 could facilitate GCV uptake and, thereby, enhance cytotoxicity in HSV-TK/GCV system. We also identified HeLa and HepG2 as cancer cell lines rich with ENBT1, and A549, HCT-15 and MCF-7 as those poor with ENBT1. Accordingly, HSV-TK/GCV system was effective in inducing cytotoxicity in the former but not in the latter. Thus, ENBT1 was found to be a GCV transporter that could enhance the performance of HSV-TK/GCV suicide gene therapy.

Introduction

A suicide gene therapy using herpes simplex virus thymidine kinase (HSV-TK) with ganciclovir (GCV) has been under development as a tumor-targeted therapy for about 30 years (Moolten et al., 1990; Smythe et al., 1994; Simonato et al., 2013). This HSV-TK/GCV system utilizes GCV as an antitumor agent that can be activated by a series of metabolic transformation processes initiated by its phosphorylation by HSV-TK, which is transfected specifically into tumor cells in advance. HSV-TK initiates the activation of GCV by converting it to GCV monophosphate, which then undergoes phosphorylation by host cell kinases to GCV diphosphate and further to GCV triphosphate. GCV triphosphate is the cytotoxic entity that induces apoptosis of the tumor cells by being incorporated into replicating DNA and thereby arresting DNA synthesis (Reardon, 1989; Fischer et al., 2005). Therefore, the targeted and efficient transfection of the HSV-TK gene into tumor cells is prerequisite in this therapy to induce the cytotoxic effect of GCV specifically in tumor cells, while avoiding unwanted GCV-induced cytotoxicity in normal tissues and cells. To realize that, research efforts have been mainly focused on the delivery of the HSV-TK gene into tumor cells.

Provided that targeted HSV-TK gene delivery could be achieved, it is also prerequisite for GCV to enter tumor cells to induce its cytotoxic effect. However, the mechanism of its cellular entry and its impact on the HSV-TK/GCV system for cancer therapy have not been clarified (Gynther et al., 2015). It has been presumed that transporters are needed for the efficient cellular entry of GCV, because this hydrophilic drug is unlikely to be able to permeate through the cellular membrane easily by simple diffusion. Indeed, several drug transporters, such as multidrug and toxin extrusion protein 1/SLC47A1, multidrug and toxin extrusion protein 2-K/SLC47A2 (Tanihara et al., 2007), organic anion transporter 1/SLC22A6

(Takada et al., 2002), organic anion transporter 2/SLC22A7 (Cheng et al., 2012) and organic cation transporter 1/SLC22A1 (Takada et al., 2002), have been reported to mediate the transport of GCV across the cellular membrane, and suggested to be involved in its renal excretion and some other disposition processes. On the other hand, carrier-mediated transport systems for purine nucleobases have been suggested to be involved in the cellular uptake of GCV in human erythrocytes (Mahony et al., 1991) and the Statens Seruminstitut rabbit corneal epithelial cell line (Majumdar et al., 2003), and in that of 9-[(3-fluoro-1-hydroxy-2-propoxy)-methyl]guanine, a GCV analog, in C6 rat glioma cell line (Buursma et al., 2004). Based on these, we assumed in the present study that equilibrative nucleobase transporter 1 (ENBT1)/SLC43A3, a newly identified transporter specific to purine nucleobases (Furukawa et al., 2015), could be a molecular entity involved in such transport systems. ENBT1 is expressed in the liver, lung and many other tissues, and suggested to be involved in the cellular uptake of purine nucleobases, such as adenine and guanine, for subsequent salvage utilization in cooperation with salvage enzymes, adenine phosphoribosyltransferase and hypoxanthine-guanine phosphoribosyltransferase 1, respectively. It might be also possible that ENBT1 is in operation with salvage enzymes in tumor cells to help their growth and proliferation. Therefore, we also hypothesized that ENBT1 could likewise play a role in the activation of GCV in cooperation with HSV-TK by facilitating the cellular entry of GCV in HSV-TK/GCV system.

To test this hypothesis, we first assessed the transport of GCV by ENBT1 introduced into mammalian cell lines. After finding that ENBT1 is capable of transporting GCV, we assessed the cooperative function of ENBT1 with HSV-TK in GCV uptake and its activation in mammalian cell lines transfected with them. We also assessed the impact of the introduction of HSV-TK on GCV uptake and its activation in cancer cell lines with varied levels of ENBT1 expression.

Materials and Methods

Materials. [^{3}H]GCV (6.9 Ci/mmol), [^{3}H]uridine (14.7 Ci/mmol) and [^{3}H]adenine (31.5 Ci/mmol) were obtained from Moravek Biochemicals (Brea, CA). Unlabeled GCV was obtained from Wako Pure Chemical Industries (Osaka, Japan). Dulbecco's modified Eagle's medium (DMEM) and RPMI 1640 medium were obtained from Wako Pure Chemical Industries and Sigma-Aldrich (St. Louis, MO), respectively. All other reagents were of analytical grade and commercially obtained.

Cell Culture. HEK293, MDCKII, HeLa, HepG2, A549, HCT-15 and MCF-7 cells were obtained from Cell Resource Center for Biomedical Research, Tohoku University, Japan. All these cells were maintained at 37°C and 5% CO_2 in a growth medium (RPMI 1640 medium for HCT-15 cells and DMEM for the others) supplemented with 10% fetal bovine serum (FBS), 100 units/ml penicillin, and 100 μg/ml streptomycin.

Preparation of Plasmids. The plasmids carrying the cDNA of human ENBT1/SLC43A3 (GenBank accession number, NM_017611.2) were those prepared in our previous study (Furukawa et al., 2015). One plasmid had the SLC43A3 cDNA incorporated into the pCI-neo vector (Promega, Madison, WI), and another with the cDNA incorporated into the pEGFP-C1 vector (Clontech Laboratories, Mountain View, CA) for the generation of ENBT1 tagged with GFP (GFP-ENBT1).

For the preparation of a plasmid carrying the cDNA of human equilibrative nucleoside transporter 1 (ENT1)/SLC29A1, its cDNA was cloned by an RT-PCR method, using the primers designed on the basis of the sequence in GenBank under the accession number of NM_001078175.2. The RT reaction was carried out to obtain cDNA mixture, using 1 μg of the total human brain RNA, an oligo(dT) primer, and ReverTra Ace (Toyobo, Osaka, Japan) as a reverse transcriptase. The open reading frame region of its cDNA was amplified by PCR

using PrimeStar Max DNA polymerase (Takara Bio, Shiga, Japan) and the following primers: forward primer, 5'-CAG GGA AAA CCG AGA ACA CCA T-3'; reverse primer, 5'-ACT CAA GCA AAT GCC GAG GCT A-3'. The second PCR was carried out using the PCR product as a template and a forward primer containing a XhoI restriction site (underlined), 5'-GAC CTC GAG CCA TGA CAA CCA GTC ACC AG-3', and a reverse primer containing an XbaI restriction site (underlined), 5'-CAA TCT AGA GTC ACA CAA TTG CCC GGA AC-3'. Both PCR reactions were performed using the following conditions: predenature at 94^{o}C for 2 min, and 33 cycles of 1) denature at 98^{o}C for 10 s, 2) annealing at 55^{o}C for 5 s, and 3) extension at 72^{o}C for 10 s. The amplified product was digested with the indicated restriction enzymes and incorporated into pCI-neo vector. The sequence of the final product was determined with an automated sequencer (ABI PRISM 3100; Applied Biosystems, Foster City, CA).

The cDNA of human ENT2/SLC29A2 (GenBank accession number, NM_001300868.1) was similarly cloned by the RT-PCR method and incorporated into pCI-neo vector to prepare a plasmid carrying the cDNA. The forward and reverse primers for the initial PCR were 5'-ACC AGT GCT GCC CCT ACA GA-3' and 5'-ACC CTT TCC ATG AGG TCT TGT GC-3', respectively. The primers for the second PCR were as follows: forward primer containing an EcoRI restriction site (underlined), 5'-GCA GAA TTC GGC CAT GGC GCG AGG AGA CG-3'; reverse primer containing an XbaI restriction site (underlined), 5'-GAA TCT AGA TTC AGA GCA GCG CCT TGA AG-3'. All the other procedures were the same as those for ENT1.

The coding DNA fragment for HSV-TK (GenBank accession number, AF057310.1) was obtained from Operon Biotechnologies (Tokyo, Japan), where it was synthesized and incorporated into pUC57 vector. The DNA fragment was transferred into pIRESpuro3 vector (Takara Bio), and also into pCI-neo vector together with the coding DNA fragment for FLAG

for the generation of HSV-TK tagged with FLAG (FLAG-HSV-TK).

Preparation of HEK293 Cells Transiently Expressing ENBT1, ENT1, ENT2, HSV-TK, and ENBT1 with HSV-TK. For the transient expression of ENBT1, ENT1 or ENT2, HEK293 cells (2.0×10^5 cells/ml, 1 ml/well) were seeded on 24-well plates coated with poly-L-lysine, transfected with the pCI-neo based plasmid for each transporter (1 μg/well) by using 1.5 μl/well of Lipofectamine 2000 (Invitrogen, Carlsbad, CA) as a transfection reagent, according to the manufacturer's instructions, and cultured for 48 h. Mock cells were prepared by the same transient transfection procedures, using empty pCI-neo vector.

In experiments to assess the cooperation of ENBT1 and HSV-TK, HEK293 cells were similarly transfected with 1 μg/well of total plasmids with a ratio of 1:1 for the pCI-neo-based one for ENBT1 and the pIRESpuro3-based one for HSV-TK for their co-expression. For the expression of each of them alone, a half of the total amount of plasmids was replaced with the empty vector. For the preparation of mock cells having neither ENBT1 nor HSV-TK, both plasmids were replaced with the empty vectors.

Preparation of HeLa, HepG2, A549, HCT-15 and MCF-7 Cells Transiently Expressing FLAG-HSV-TK. HeLa, HepG2, A549, HCT-15 or MCF-7 cells (1.5×10^5 cells/ml, 1 ml/well) were grown on 24-well plates for 36 h (HCT-15 cells) or 12 h (the other cells). They were then transfected with the pCI-neo-based plasmid for FLAG-HSV-TK (1 μg/well) by using 1.5 μl/well of Lipofectamine 3000 (Invitrogen) as a transfection reagent, according to the manufacturer's instructions, and cultured for 48 h for its transient expression. FLAG-HSV-TK was used to assess the level of its protein expression by probing for FLAG by western blotting, as described below.

Transient Expression of FLAG-HSV-TK and Simultaneous Silencing of ENBT1 in HeLa Cells. HeLa cells (2.5×10^5 cells/ml, 1 ml/well) were grown on 24-well plates for 6 h,

and transfected with the pCI-neo-based plasmid for FLAG-HSV-TK (1 μg/well) with or without 4 pmol/well of the siRNA specific to the mRNA of ENBT1 (Stealth Select RNAi siRNA, Thermo Fisher Scientific, Waltham, MA) by using Lipofectamine 3000 (0.75 μl/well), and cultured for 72 h for the transient expression of FLAG-HSV-TK with or without simultaneous silencing of ENBT1. The sequences of the siRNA were as follows: ENBT1 sense, 5'-AAU GUC AGA AGA AUG GCA AGC AUG A-3'; ENBT1 antisense, 5'-UCA UGC UUG CCA UUC UUC UGA CAU U-3'. For control, the siRNA was replaced with an RNA duplex unrelated to ENBT1 (Stealth RNAi Negative Control Low GC Duplex, Thermo Fisher Scientific) and the plasmid for FLAG-HSV-TK was replaced with empty pCI-neo vector.

Preparation of MDCKII Cells Stably Expressing ENBT1, GFP-ENBT1, HSV-TK, and GFP-ENBT1 with HSV-TK. MDCKII cells (4.0×10^5 cells/ml, 0.5 ml/well) were seeded on 24-well plates, transfected with the pCI-neo-based plasmid for ENBT1 or pEGFP-C1-based plasmid for GFP-ENBT1 (1 μg/well) by using 1.5 μl/well of Lipofectamine 2000, and cultured in DMEM supplemented with 10% FBS and 800 μg/ml Geneticin for 2 to 3 weeks. Antibiotic-resistant clones were selected to obtain those stably expressing ENBT1 or GFP-ENBT1.

MDCKII cells with or without stably expressing GFP-ENBT1were similarly transfected with the pIRESpuro3-based plasmid for HSV-TK by using Lipofectamine 2000, and cultured in DMEM supplemented with 10% FBS and 5 μg/ml puromycin for 2 to 3 weeks. Antibiotic-resistant clones were selected to obtain those stably expressing HSV-TK with or without GFP-ENBT1. GFP-ENBT1 was used to help confirming preliminarily by visual inspection of GFP-derived fluorescence that the transporter was not lost during the procedure for the additional introduction of HSV-TK.

Mock cells were prepared by the same stable transfection procedures, using the empty vectors.

The MDCKII cell line was chosen as an epithelial cell model to host ENBT1 as the parenchymal liver cell, which belongs to epithelial cell species, has been suggested to be a major cell species in which this transporter is expressed (Furukawa et al., 2015).

Transport Study. MDCKII cells stably expressing ENBT1, HSV-TK, GFP-ENBT1, or GFP-ENBT1 with HSV-TK (1.5×10^5 cells/ml, 1 ml/well) were grown on 24-well plates for 72 h to confluence. The cells in each well were preincubated in 1 ml of substrate-free uptake buffer (140 mM NaCl, 5 mM KCl, 0.4 mM KH_2PO_4, 0.8 mM $MgSO_4$, 1.0 mM $CaCl_2$, 25 mM glucose, and 10 mM HEPES, pH 7.4) for 5 min. Uptake assays were started by replacing the substrate-free uptake buffer for preincubation with the one containing the radioisotope-labeled substrate (0.25 ml). All of the procedures were conducted at 37°C. Assays were stopped by addition of ice-cold substrate-free uptake buffer (2 ml), and the cells were washed two times with 2 ml of the same buffer. The cells were solubilized in 0.5 ml of 0.2 M NaOH solution containing 0.5% SDS at room temperature for 1 h, and the associated radioactivity was measured by liquid scintillation counting. Cellular protein content was determined by the BCA method (BCA Protein Assay Reagent Kit; Thermo Fisher Scientific), using bovine serum albumin as the standard. Uptake assays were also conducted in mock cells to estimate nonspecific uptake.

Uptake assays were similarly conducted in all the cells transiently transfected as indicated.

The specific uptake of a substrate by ENBT1 or GFP-ENBT1 was estimated by subtracting its uptake in mock cells from that in the cells expressing the transporter.

Western Blot Analysis. HeLa, HepG2, A549, HCT-15 and MCF-7 cells transiently transfected with FLAG-HSV-TK, and HeLa cells transfected with FLAG-HSV-TK with or without simultaneous silencing of ENBT1 were washed twice with ice-cold phosphate buffered saline (pH 7.4), and then lysed with an ice-cold buffer (pH 7.4) containing 4 M urea,

10 mM NaCl, 50 mM Tris-HCl, 1 mM EDTA and 1% SDS, and supplemented with protease inhibitor cocktail (Sigma-Aldrich). The lysed sample was centrifuged at 10,000 × g for 10 min at 4°C, and the resultant supernatant was used as the sample of the whole cell lysate after the addition of 2 × sample buffer (pH 6.8) containing 100 mM Tris-HCl, 4% lithium dodecyl sulfate, 50 mM dithiothreitol and 0.2% bromophenol blue. The sample (30 μg) was separated on the 10% SDS-polyacrylamide gel by electrophoresis and transferred to Immun-Blot polyvinylidene difluoride membrane (Bio-Rad Laboratories, Hercules, CA). The membrane was blocked with 5% skim milk in Tris-buffered saline (pH 7.4) containing 0.1% Tween 20 and then probed with the primary antibodies of rabbit anti-ENBT1/SLC43A3 polyclonal antibody (Atlas Antibodies, Stockholm, Sweden) and mouse anti-FLAG monoclonal antibody (Sigma-Aldrich) at a dilution of 1:200 and 1:2,000, respectively, for overnight at 4°C. After washing three times with Tris-buffered saline (pH 7.4) containing 0.1% Tween 20, the membrane was incubated with the secondary antibodies of horseradish peroxidase-conjugated goat anti-rabbit IgG (Jackson ImmunoResearch Laboratories, West Grove, PA) and horseradish peroxidase-conjugated goat anti-mouse IgG (Sigma-Aldrich), respectively, for the detection of ENBT1 and FLAG-HSV-TK at a dilution of 1:10,000 for 1 h at room temperature. Then, the expression levels of ENBT1 and FLAG-HSV-TK were determined by enhanced chemiluminescence using Immobilon Western (EMD Millipore, Billerica, MA), according to the manufacturer's instructions.

For the detection of β-actin, mouse anti-β-actin antibody (Sigma-Aldrich) was used as the primary antibody at a dilution of 1:1000 and, thereafter, the sample was processed by the same procedures as those for the detection of FLAG-HSV-TK.

Cell Viability Assay. MDCKII cells stably expressing GFP-ENBT1 and/or HSV-TK (8.0×10^5 cells/ml, 0.1 ml/well) were grown on 96-well plates for 4 h, and then incubated for 72 h in 0.1 ml of DMEM in the presence of GCV at varied concentrations or in its absence.

The cell viability was evaluated in phenol red-free DMEM by the WST-8 assay using Cell Counting Kit-8 (Dojindo Laboratories, Kumamoto, Japan), according to the manufacturer's instructions. In the assay, the photometric absorbance at 450 nm was determined as a measure of the cell viability, using a plate reader (ARVO MX multilabel counter, PerkinElmer, Waltham, MA) for the detection of WST-8 formazan produced by live cells, and normalized to that observed in the absence of GCV.

HeLa, HepG2, A549, HCT-15 and MCF-7 cells (1.5×10^5 cells/ml, 1 ml/well) were grown on 24-well plates for the transient introduction of FLAG-HSV-TK. The cells were, after transfection with the plasmid for FLAG-HSV-TK, incubated in 1 ml of a growth medium (RPMI 1640 for HCT-15 cells and DMEM for the other cells) for 68 h in the presence of GCV (30 μM) or in its absence, before being assessed for their viability by using Cell Counting Kit-8.

HeLa cells (2.5×10^5 cells/ml, 1 ml/well) were grown on 24-well plates for the transient introduction of FLAG-HSV-TK with or without simultaneous silencing of ENBT1. The cells were, after transfection with the plasmid for FLAG-HSV-TK with or without siRNA for silencing ENBT1, incubated in 1 ml of DMEM for 8 h in the absence of GCV and, then, 72 h in the presence of GCV (30 μM) or in its absence, before being assessed for their viability by using Cell Counting Kit-8.

Data Analysis. The saturable uptake of GCV was analyzed by assuming Michaelis-Menten type carrier-mediated transport represented by the following equation: $v = V_{max} \times s/(K_m + s)$. GCV is the substrate in this analysis, and the parameters of the maximum transport rate (V_{max}) and the Michaelis constant (K_m) were estimated by fitting this equation to the profile of the uptake rate (v) *versus* the substrate concentration (s), using a non-linear least-squares regression analysis program, WinNonlin (Pharsight, Mountain View, CA).

The inhibition of adenine uptake by GCV was analyzed by using the following equation

for v as a function of the inhibitor concentration (i) at s much smaller than K_m ($s << K_m$): $v = v_0/(1 + (i/IC_{50})^n)$. Adenine and GCV are the substrate and inhibitor, respectively, in this analysis, and the half inhibition concentration (IC_{50}) of GCV was estimated together with the Hill coefficient (n) and v in the absence of the inhibitor (v_0) by fitting this equation to the profile of *v versus i*. We here assumed the ordinary competitive inhibition model, in which the specific uptake of a test substrate can be completely inhibited by another substrate that acts as a competitive inhibitor, as GCV, which was identified as a substrate in the present study, could be such a competitive inhibitor.

Data are presented as the means ± S.E. from multiple experiments conducted in a single determination or duplicate. Statistical analysis was performed by using Student's *t* test or, when multiple comparisons were needed, analysis of variance (ANOVA) followed by Dunnett's test, with $P < 0.05$ considered significant.

JPET Fast Forward. Published on November 2, 2016 as DOI: 10.1124/jpet.116.236984
This article has not been copyedited and formatted. The final version may differ from this version.

Results

GCV Transport by ENBT1. We first assessed the uptake of [^{3}H]GCV in HEK293 cells transiently expressing ENBT1 and, as shown in Fig. 1, found that it was much greater than its uptake in mock cells, indicating that ENBT1 can transport GCV efficiently. On the other hand, [^{3}H]GCV uptake was not increased, compared with that in mock cells, in cells expressing ENT1 and those expressing ENT2, suggesting that they cannot transport GCV, although they can reportedly transport some nucleobases (Yao et al., 2002; Yao et al,, 2011). The operation of transiently introduced ENT1 and ENT2 in the present study was confirmed by significant increases in the uptake of [^{3}H]uridine (10 nM) as a probe substrate in ENT1-expressing cells (337 ± 13 fmol/mg protein) and ENT2-expressing cells (346 ± 7 fmol/mg protein), compared with that in mock cells (246 ± 3 fmol/mg protein), where data of the initial 1-min uptake are presented as means ± S.E. from 4 experiments conducted in a single determination.

For more detailed analysis of GCV transport by ENBT1, we prepared MDCKII cells stably expressing ENBT1. The uptake of [^{3}H]GCV at a trace concentration of 60 nM was in proportion to time up to 40 s in the cells expressing ENBT1 and also in mock cells, as shown in Fig. 2A. Based on that, the uptake period was set to be 40 s to evaluate the initial rate of its uptake in subsequent experiments. Kinetic analysis indicated that the specific uptake of [^{3}H]GCV by ENBT1 was saturable, conforming to the Michaelis-Menten kinetics with a K_m of 2.75 mM and a V_{max} of 6.58 nmol/min/mg protein (Fig. 2B). For comparison with the K_m, the IC_{50} of GCV for the uptake of [^{3}H]adenine by ENBT1 was evaluated at the adenine concentration of 5 nM, which was in the linear phase of its transport kinetics with the apparent K_m of 0.94 μM (Furukawa et al., 2015). If a metabolic enzyme might be in cooperation to facilitate the uptake of [^{3}H]GCV by ENBT1, the K_m would be modulated to be apparently deviated from the IC_{50} as an alternative measure of the affinity of GCV for ENBT1,

JPET Fast Forward. Published on November 2, 2016 as DOI: 10.1124/jpet.116.236984
This article has not been copyedited and formatted. The final version may differ from this version.

as we previously reported for [^{3}H]adenine uptake (Furukawa et al., 2015). However, the IC_{50} was estimated to be 1.67 mM (Fig. 3), being comparable with the K_m of [^{3}H]GCV uptake and, hence, suggesting that MDCKII cells do not have any metabolic enzyme that can cooperate with ENBT1 in [^{3}H]GCV uptake.

Cooperation of ENBT1 with HSV-TK in the Uptake and Activation of GCV. The uptake of [^{3}H]GCV was only modest in mock HEK293 and MDCKII cells (Figs. 1 and 2A), suggesting that the operation of any native GCV transporter could be negligible. We assumed that the uptake of GCV could be insufficient to induce its cytotoxic effect in such cells, even when transfected with HSV-TK for its activation. To examine that assumption and the potential role of ENBT1 in the uptake and activation of GCV in cooperation with HSV-TK, we first assessed the effect of the transient introduction of ENBT1 and/or HSV-TK on the uptake of [^{3}H]GCV in HEK293 cells. As shown in Fig. 4, although the uptake of [^{3}H]GCV (60 nM) for a 5-min period was unchanged when only HSV-TK was introduced into the cells, it was increased by the introduction of ENBT1 modestly and further more by the introduction of HSV-TK together with ENBT1, suggesting the cooperation of ENBT1 with HSV-TK in [^{3}H]GCV uptake. It is most likely because HSV-TK maintains the concentration of [^{3}H]GCV low by metabolizing it within the cells, and thereby has its ENBT1-mediated facilitative influx sustained. This could bring about the additional increase in [^{3}H]GCV uptake, which is represented by the amount of ^{3}H-labeled GCV and its metabolites accumulated within the cells, and it could be associated with the metabolic activation of GCV for the induction of its cytotoxic effect.

To further confirm the cooperation of ENBT1 with HSV-TK in [^{3}H]GCV uptake and also to examine its impact on GCV activation for the induction of its cytotoxic effect, we conducted a series of experiments using MDCKII cells stably expressing GFP-ENBT1 and/or HSV-TK. Similarly to the results in HEK293 cells having transiently introduced ENBT1

and/or HSV-TK, [^{3}H]GCV uptake was increased, compared with that in mock cells, in cells having GFP-ENBT1, but not in those having HSV-TK alone, after the initial 5-min and extended 60-min uptake periods (Fig. 5). An increase in [^{3}H]GCV uptake by the introduction of HSV-TK in addition to GFP-ENBT1 was confirmed after the extended 60-min uptake period (Fig. 5B). Although GFP-ENBT1 was previously demonstrated to be almost exclusively localized to the basolateral membrane in polarized MDCKII cells (Furukawa et al., 2015), it was uniformly distributed in the plasma membrane, as generally expected, in nonpolarized MDCKII cells used in the present study (data not shown). Similarly, ENBT1, which was previously demonstrated to be localized to the basolateral membrane in human parenchymal liver cells (Furukawa et al., 2015), could be assumed to be uniformly distributed in the plasma membrane in nonpolarized MDCKII cells in some other experiments in the present study.

The cytotoxic effect induced by GCV was assessed by evaluating the viability of the cells after 72 h of incubation in the presence of GCV at varied concentrations (Fig. 6). The cell viability was found to decrease only in the cells expressing GFP-ENBT1 and HSV-TK together in a manner depending on GCV concentration, manifesting cytotoxicity induced by GCV, which was supposed to be taken up and activated by their cooperation. The cytotoxicity reached the maximum level at the GCV concentration of 30 μM, which is within the range expected to be clinically effective in HSV-TK/GCV therapy (Sangro et al., 2010). On the other hand, GCV-induced cytotoxicity was insignificant in the cells expressing GFP-ENBT1 or HSV-TK alone, as well as in mock cells.

Kinetic analysis of [^{3}H]GCV uptake by GFP-ENBT1 in cooperation with HSV-TK was conducted for its uptake rate evaluated for the initial 30-min period, which was within the range where the uptake was in proportion to time in cells expressing GFP-ENBT1 and HSV-TK together, being much greater than its uptake in mock cells (Fig. 7A). As shown in

JPET Fast Forward. Published on November 2, 2016 as DOI: 10.1124/jpet.116.236984
This article has not been copyedited and formatted. The final version may differ from this version.

Fig. 7B, [^{3}H]GCV uptake was saturable, conforming to the Michaelis-Menten kinetics with an apparent K_m of 96.7 μM. Compared with that for ENBT1-medaited transport in Fig. 2B, the apparent K_m was about 20 times smaller. It is notable that the apparent K_m was comparable with those of 47.6 μM (Hinds et al., 2000) and 69 μM (Kokoris and Black, 2002) reported for the metabolism of GCV by HSV-TK and, hence, it is likely that GCV uptake is rate-limited by the metabolic process, similarly to nucleobase uptake observed in our previous study (Furukawa et al., 2015).

Impact of ENBT1 Level on the Performance of HSV-TK/GCV System in Cancer Cell Lines. Based on the finding that ENBT1 plays a critical role as a pathway of GCV entry into the cells in the manifestation of GCV-induced cytotoxicity, we predicted that the performance of HSV-TK/GCV system depends on the level of ENBT1 expressed in target cells. To examine that possibility, we evaluated the level of constitutively expressed ENBT1 and the performance of HSV-TK/GCV system in various human cancer cell lines for comparison. Among 5 cell lines tested for the expression of ENBT1 protein by western blotting, it was abundantly expressed in HeLa and HepG2, whereas it was not detectable in A549, HCT-15 and MCF7 (Fig. 8). Based on that, we categorized the former as ENBT1-rich cell lines and the latter as ENBT1-poor ones. ENBT1 has the predicted molecular mass of about 55 kDa, which corresponds to the band observed at around 50 kDa in the HeLa and HepG2 cell lines. In addition to that, a secondary band was observed in a higher molecular weight range in each cell line. It may suggest the presence of a post-transcriptionally modulated ENBT1. The expression of transiently introduced FLAG-HSV-TK was, on the other hand, confirmed in all the cell lines (Fig. 8). Reflecting the levels of ENBT1 expression, the uptake of [^{3}H]GCV (30 μM), which was evaluated for a 5-min uptake period, was greater in ENBT1-rich cell lines (Fig. 9A) than in ENBT1-poor ones (Fig. 9B). Furthermore, [^{3}H]GCV uptake was increased by the transient introduction of FLAG-HSV-TK only in

ENBT1-rich cell lines, suggesting its efficient cooperation with abundant ENBT1 in increasing [^{3}H]GCV uptake. Consistent with the suggestion in the preceding section that the increase in [^{3}H]GCV uptake could be associated with the metabolic activation of GCV for the induction of its cytotoxic effect, GCV-induced cytotoxicity was induced by the introduction of FLAG-HSV-TK in ENBT1-rich cell lines, as indicated by the significantly lower cell viability in FLAG-HSV-TK-transfected cells than in mock cells (Fig. 10A), whereas such inductions of GCV-induced cytotoxicity were insignificant or only modest in ENBT1-poor cell lines (Fig. 10B). Slight decreases in the cell viability were observed in mock cells of the HeLa, HepG2 and MCF-7 cell lines. It may suggest the presence of a minor HSV-TK-independent mechanism to induce the cytotoxic effect of GCV in those cell lines. This effect may be independent of the cellular uptake of GCV, because it was observed in the MCF-7 cell line, which was identified to be poor with ENBT1, and [^{3}H]GCV uptake in this cell line was not increased by the introduction of FLAG-HSV-TK, suggesting that there is not any alternative transporter that can facilitate the cellular uptake of GCV. In those cell lines, GCV may act on the cellular surface to induce the minor cytotoxic effect.

To further verify the role of ENBT1 in inducing GCV-induced cytotoxicity by facilitating the uptake and activation of GCV in HSV-TK/GCV system, we examined the effect of the silencing of ENBT1 on [^{3}H]GCV uptake and GCV-induced cytotoxicity in HeLa cells. As shown in Fig. 11A, the expression of ENBT1 protein was almost completely suppressed by RNA interference using the siRNA specific to the mRNA of ENBT1 in HeLa cells with or without transiently introduced FLAG-HSV-TK, indicating successful ENBT1 silencing. Accordingly, an increase in [^{3}H]GCV uptake induced by the transient introduction of FLAG-HSV-TK was suppressed by the silencing of ENBT1 (Fig. 11B), indicating its cooperative role in that FLAG-HSV-TK-induced increase in [^{3}H]GCV uptake. As shown in Fig. 11C, GCV-induced cytotoxicity, represented by a decrease in the cell viability, was

induced by the introduction of FLAG-HSV-TK and it was suppressed by the silencing of ENBT1, indicating its role in coordinated GCV activation for the induction of cytotoxicity. It is also notable that the introduction of FLAG-HSV-TK in ENBT1-silenced cells did not induce either any significant increase in [^{3}H]GCV uptake (Fig. 11B) or any significant GCV-induced cytotoxicity (Fig. 11C), supporting the suggested cooperative role of ENBT1. This result also suggests that there is no other transporter that can significantly facilitate GCV uptake for the induction of its cytotoxic effect in cooperation with HSV-TK in HeLa cells. It is most likely that similarly abundant ENBT1 in HepG2 cells could be likewise responsible for GCV uptake and involved in eliciting GCV-induced cytotoxicity, although we cannot fully exclude a possibility that some other GCV transporters might also be involved in part. The increase in [^{3}H]GCV uptake induced by FLAG-HSV-TK and the GCV-induced cytotoxicity in FLAG-HSV-TK-transfected cells in this set of experiments that involves ENBT1 silencing procedures in HeLa cells were not as much as those observed in HeLa cells in another set of experiments in Fig. 10. Although the mechanism that caused these differences are unknown, the silencing procedures may have something to do with that. However, the effects of ENBT1 silencing on [^{3}H]GCV uptake and GCV-induced cytotoxicity in FLAG-HSV-TK-transfected cells were evident, indicating the critical role of ENBT1 in those processes.

JPET Fast Forward. Published on November 2, 2016 as DOI: 10.1124/jpet.116.236984
This article has not been copyedited and formatted. The final version may differ from this version.

Discussion

The present study has successfully demonstrated that GCV is a substrate of ENBT1, a purine nucleobase-specific transporter that has recently been identified. Nucleobase-specific carrier-mediated transport systems have been suggested to be involved in GCV uptake in human erythrocytes (Mahony et al., 1991) and the Statens Seruminstitut rabbit corneal epithelial cell line (Majumdar et al., 2003), with the K_m values of 0.89 mM and 1.29 mM, respectively. Those K_m values are fairly close to that of ENBT1 (2.75 mM), suggesting its role as the transporter responsible for those transport systems. Although a nucleoside transport system has also been suggested to be involved in part in GCV uptake in erythrocytes, its affinity for GCV is reportedly much lower with a K_m of 14 mM (Mahony et al., 1991).

The apparent K_m of nucleobase uptake in ENBT1-expressing MDCKII cells has been previously suggested to represent the affinity of the nucleobase for its specific salvage enzyme, by which the metabolism limits the rate of overall uptake process cooperatively mediated by ENBT1 and the salvage enzyme (Furukawa et al., 2015). This was based on findings that, typically, the apparent K_m of [^{3}H]adenine uptake (0.94 μM) was comparable with the K_m of adenine phosphoribosyltransferase, the adenine-specific salvage enzyme, for adenine (0.6 - 0.9 μM) and, in addition, it was smaller than the IC_{50} of adenine (13 μM) for [^{3}H]guanine uptake in ENBT1-expressing cells, where the IC_{50} could represent the affinity of adenine to ENBT1 as this nucleobase acts on ENBT1 as an inhibitor of [^{3}H]guanine transport but not on hypoxanthine-guanine phosphoribosyltransferase 1, the guanine-specific salvage enzyme. However, the IC_{50} of GCV for [^{3}H]adenine uptake (1.67 mM) was found to be comparable with the K_m of [^{3}H]GCV uptake (2.75 mM). This could be because the K_m for [^{3}H]GCV, which is unlikely to undergo any significant metabolism in the canine cells, could represent its affinity to ENBT1. Any modulation of the IC_{50} is also unlikely, as GCV, which is

a guanine analog, is not likely to act on adenine phosphoribosyltransferase as an inhibitor, based on a study indicating that 2-amino substitution together with substitution with anything other than amino group at position 6 in the purine structure, which is maintained in GCV as in guanine, markedly diminishes the binding of purine derivatives to the enzyme (Krenitsky et al., 1969). It is notable that the K_m for [^{3}H]GCV is about one to two orders of magnitude greater than the IC_{50} values of adenine (13 μM), guanine (70 μM) and hypoxanthine (350 μM) for ENBT1 (Furukawa et al., 2015), suggesting that GCV has a lower affinity to ENBT1 than those major nucleobases.

It was also demonstrated that ENBT1 could cooperate with HSV-TK in facilitating the uptake and activation of GCV for the induction of its cytotoxic effect in HSV-TK/GCV system. In a series of experiments using MDCKII cells to assess that cooperation, it was shown that GCV could induce cytotoxicity only in the cells having stably introduced GFP-ENBT1 together with HSV-TK (Fig. 6). Notably, GCV-induced cytotoxicity was insignificant in the cells having HSV-TK alone, as well as in mock cells and cells having ENBT1 alone. It is also notable that GCV uptake was, compared with that in mock cells, unchanged in the cells having HSV-TK alone, increased only modestly in those having GFP-ENBT1 alone and increased further more in those having both of them together. It is evident from these results that HSV-TK/GCV system cannot work effectively without ENBT1, which provides a pathway of GCV entry into the cells, or alternatively GCV transporters that could work similarly in cooperation with HSV-TK. In another series of experiments using cancer cell lines, transiently introduced FLAG-HSV-TK could induce GCV-induced cytotoxicity in ENBT1-rich ones, but not in ENBT1-poor ones (Figs. 8 and 10). Accordingly, GCV uptake was greater in the former than in the latter in the absence of HSV-TK and was increased by HSV-TK introduction in the former, but not in the latter (Fig. 9). Furthermore, the GCV-induced cytotoxicity and the increase in GCV uptake induced by HSV-TK

introduction in the HeLa cell line, an ENBT1-rich one, were suppressed by the silencing of ENBT1 (Fig. 11). These results further support the suggested role of ENBT1 in cooperation with HSV-TK in the uptake and activation of GCV in HSV-TK/GCV system and also indicate that the ENBT1-rich tumors, if identified, could be effectively treated with the HSV-TK/GCV system. Thus, ENBT1 could play a critical role in having HSV-TK/GCV system work effectively for cancer therapy.

Although the impact of ENBT1 on the performance of HSV-TK/GCV system remains to be demonstrated *in vivo*, it is reported in a study using nude mice that the growth of transplanted cells of HSV-TK-transfected HepG2, which was identified as an ENBT1-rich cell line in this study, was suppressed by GCV treatment after introduction of HSV-TK (Ishikawa et al., 2001). Likewise, in the clinical practice of HSV-TK/GCV suicide gene therapy, identifying tumors rich with ENBT1 would help selecting the patients for whom this therapy could be effective. As an example, it is reported that an increased expression of ENBT1 mRNA was observed in thyroid cancer developed in patients exposed to radioactive iodine (Abend et al., 2012). On the other hand, it has more recently been reported that a phase III study using adenovirus-mediated gene therapy with HSV-TK/GCV system in glioblastoma patients failed to improve overall survival, although it could prolong their median time to death or re-intervention (Westphal et al., 2013). This might be a case suggesting a possibility that the expression of ENBT1 or any other transporter that can transport GCV is not high enough in glioma cells to facilitate GCV uptake efficiently for eliciting sufficient GCV-induced cytotoxicity. If that might be the case, such a situation could be improved by enhancing GCV delivery into the glioma cells expressing HSV-TK. The targeted delivery of the ENBT1 gene with the HSV-TK gene into tumor cells could be a strategy to explore to improve the performance of HSV-TK/GCV suicide gene therapy by enhancing GCV delivery.

In conclusion, we have successfully identified ENBT1 as a GCV transporter and

demonstrated that ENBT1 can play an important role in the manifestation of the GCV-induced cytotoxicity of HSV-TK/GCV system for cancer therapy.

Authorship Contributions

Participated in research design: Furukawa, Inoue, Ohta, Yasujima, Yuasa

Conducted experiments: Furukawa, Mimura

Performed data analysis: Furukawa, Inoue

Wrote or contributed to the writing of the manuscript: Furukawa, Inoue, Yuasa

References

Abend M, Pfeiffer RM, Ruf C, Hatch M, Bogdanova TI, Trouko MD, Riecke A, Hartmann J, Meineke V, Boukheris H, Sigurdson AJ, Mabuchi K, and Brenner AV (2012) Iodine-131 dose dependent gene expression in thyroid cancers and corresponding normal tissues following the Chernobyl accident. *PLOS One* **7**: e39103.

Buursma AR, van Dillen IJ, van Waarde A, Vaalburg W, Hospers GA, Mulder, NH, and de Vries EF (2004) Monitoring HSVtk suicide gene therapy: the role of [^{18}F]FHPG membrane transport. *Br J Cancer* **91**: 2079-2085.

Cheng Y, Vapurcuyan A, Shahidullah M, Aleksunes LM, and Pelis RM (2012) Expression of organic anion transporter 2 in the human kidney and its potential role in the tubular secretion of guanine-containing antiviral drugs. *Drug Metab Dispos* **40**: 617-624.

Fischer U, Steffens S, Frank S, Rainov NG, Schulze-Osthoff K, and Kramm CM (2005) Mechanisms of thymidine kinase/ganciclovir and cytosine deaminase/5-fluorocytosine suicide gene therapy-induced cell death in glioma cells. *Oncogene* **24**: 1231-1243.

Furukawa J, Inoue K, Maeda J, Yasujima T, Ohta K, Kanai Y, Takada T, Matsuo H, and Yuasa H (2015) Functional identification of SLC43A3 as an equilibrative nucleobase transporter involved in purine salvage in mammals. *Sci Rep* **5**: 15057.

Gynther M, Kääriäinen TM, Hakkarainen JJ, Jalkanen AJ, Petsalo A, Lehtonen M, Peura L, Kurkipuro J, Samaranayake H, Ylä-Herttuala S, Rautio J, and Forsberg MM (2015) Brain pharmacokinetics of ganciclovir in rats with orthotopic BT4C glioma. *Drug Metab Dispos* **43**: 140-146.

Hinds TA, Compadre C, Hurlburt BK, and Drake RR (2000) Conservative mutations of glutamine-125 in herpes simplex virus type 1 thymidine kinase results in a ganciclovir kinase with minimal deoxypyrimidine kinase activities. *Biochemistry* **39**: 4105-4111.

Ishikawa H, Nakata K, Mawatari F, Ueki T, Tsuruta S, Ido A, Nakao K, Kato Y, Ishii N, and Eguchi K (2001) Retrovirus-mediated gene therapy for hepatocellular carcinoma with reversely oriented therapeutic gene expression regulated by α-fetoprotein enhancer/promoter. *Biochem Biophys Res Commun* **287**: 1034-1040.

Krenitsky TA, Neil SM, Elion GB, and Hitchings GH (1969) Adenine phosphoribosyltransferase from monkey liver: specificity and properties. *J Biol Chem* **244**: 4779-4784.

Kokoris MS, and Black ME (2002) Characterization of herpes simplex virus type 1 thymidine kinase mutants engineered for improved ganciclovir or acyclovir activity. *Protein Sci* **11**: 2267-2272.

Mahony WB, Domin BA, and Zimmerman TP (1991) Ganciclovir permeation of the human erythrocyte membrane. *Biochem Pharmacol* **41**: 263-271.

Majumdar S, Tirucherai GS, Pal D, Mitra AK (2003) Functional differences in nucleoside and nucleobase transporters expressed on the rabbit corneal epithelial cell line (SIRC) and isolated rabbit cornea. *AAPS PharmSci* **5**: E15.

Moolten FL, Wells JM, Heyman RA, and Evans RM (1990) Lymphoma regression induced by ganciclovir in mice bearing a herpes thymidine kinase transgene. *Hum Gene Ther* **1**: 125-134.

Reardon JE (1989) Herpes simplex virus type 1 and human DNA polymerase interactions with 2'-deoxyguanosine 5'-triphosphate analogues. Kinetics of incorporation into DNA and induction of inhibition. *J Biol Chem* **264**: 19039-19044.

Sangro B, Mazzolini G, Ruiz M, Ruiz J, Quiroga J, Herrero I, Qian C, Benito A, Larrache J, Olagüe C, Boan J, Peñuelas I, Sádaba B, and Prieto J (2010) A phase I clinical trial of thymidine kinase-based gene therapy in advanced hepatocellular carcinoma. *Cancer Gene Ther* **17**: 837-843.

Simonato M, Bennett J, Boulis NM, Castro MG, Fink DJ, Goins WF, Gray SJ, Lowenstein PR, Vandenberghe LH, Wilson TJ, Wolfe JH, and Glorioso JC (2013) Progress in gene therapy for neurological disorders. *Nat Rev Neurol* **9**: 277-291.

Smythe WR, Hwang HC, Amin KM, Eck SL, Davidson BL, Wilson JM, Kaiser LR, and Albelda SM (1994) Use of recombinant adenovirus to transfer the herpes simplex virus thymidine kinase (HSVtk) gene to thoracic neoplasms: an effective in vitro drug sensitization system. *Cancer Res* **54**: 2055-2059.

Takada M, Khamdang S, Narikawa S, Kimura H, Kobayashi Y, Yamamoto T, Cha SH, Sekine T, and Endou H (2002) Human organic anion transporters and human organic cation transporters mediate renal antiviral transport. *J Pharmacol Exp Ther* **300**: 918-924.

Tanihara Y, Masuda S, Sato T, Katsura T, Ogawa O, and Inui K (2007) Substrate specificity of MATE1 and MATE2-K, human multidrug and toxin extrusions/H^+-organic cation antiporters. *Biochem Pharmacol* **74**: 359-371.

Westphal M, Ylä-Herttuala S, Martin J, Warnke P, Menei P, Eckland D, Kinley J, Kay R, Ram Z, and ASPECT Study Group (2013) Adenovirus-mediated gene therapy with sitimagene ceradenovec followed by intravenous ganciclovir for patients with operable high-grade glioma (ASPECT): a randomized, open-label, phase 3 trial. *Lancet Oncol* **14**: 823-833.

Yao SYM, Ng AML, Cass CE, Baldwin SA, and Young JD (2011) Nucleobase transport by human equilibrative nucleoside transporter 1 (hENT1). *J Biol Chem* **286**: 32552-32562.

Yao SYM, Ng AML, Vickers MF, Sundaram M, Cass CE, Baldwin SA, and Young JD (2002) Functional and molecular characterization of nucleobase transport by recombinant human and rat equilibrative nucleoside transporters 1 and 2. Chimeric constructs reveal a role for the ENT2 helix 5-6 region in nucleobase translocation. *J Biol Chem* **277**: 24938-24948.

Footnotes

This work was supported in part by a Grant-in-Aid for Scientific Research (C) from the Japan Society for the Promotion of Science (#15K08082).

Figure Legends

Fig. 1. The uptake of GCV in HEK293 cells transiently expressing ENBT1, ENT1 and ENT2. The uptake of [^{3}H]GCV (60 nM) was evaluated for 5 min at 37°C and pH 7.4. Data are presented as the means ± S.E. from 4 experiments conducted in a single determination. *P < 0.05 compared with the value for mock cells, as assessed by ANOVA followed by Dunnett's test.

Fig. 2. Kinetic analysis of the uptake of GCV by ENBT1 stably expressed in MDCKII cells. (A) Time course of the uptake of [^{3}H]GCV (60 nM) at 37°C and pH 7.4. The specific uptake estimated by subtracting the uptake in mock cells from that in cells expressing ENBT1 was evaluated in the initial phase with shorter intervals in separate experiments and shown in the inset panel. Data are presented as the means ± S.E. from 4 experiments conducted in a single determination. (B) Concentration dependence of the ENBT1-specific uptake rate of [^{3}H]GCV for 40 s at 37°C and pH 7.4. The specific uptake rate was estimated by subtracting the uptake rate in mock cells from that in cells expressing ENBT1. Data are presented as the means ± S.E. from 5 experiments conducted in a single determination. The K_m and V_{max} are 2.75 ± 0.39 mM and 6.58 ± 0.93 nmol/min/mg protein, respectively, as the means ± S.E. from 5 experimental profiles of the uptake rate *versus* concentration.

Fig. 3. Effect of GCV on adenine uptake by ENBT1 stably expressed in MDCKII cells. The inhibitory effect of GCV on the ENBT1-specific uptake rate of [^{3}H]adenine (5 nM) was evaluated for 40 s at 37°C and pH 7.4 in the presence of varied concentrations of GCV or in its absence (control). The specific uptake rate was estimated by subtracting the uptake rate in mock cells from that in cells expressing ENBT1. The observed control value for

normalization of the uptake rate was 0.234 ± 0.005 pmol/min/mg protein. Data are presented as the means ± S.E. from 4 experiments conducted in a single determination. The parameters of IC_{50}, the Hill coefficient (n) and the uptake rate in the absence of GCV (v_0) are 1.67 ± 0.12 mM, 0.79 ± 0.04 and 0.231 ± 0.003 pmol/min/mg protein, respectively, as the computer-fitted parameters with S.E. The ordinary competitive inhibition model, in which the specific uptake rate of adenine approaches null at infinite GCV concentration because of its complete inhibition, was assumed in this analysis.

Fig. 4. Effect of transient expression of ENBT1 and/or HSV-TK on GCV uptake in HEK293 cells. The uptake of [^{3}H]GCV (60 nM) was evaluated for 5 min at 37°C and pH 7.4. HEK293 cells were transiently transfected with the pCI-neo-based plasmid for ENBT1 and the pIRESpuro3-based plasmid for HSV-TK with 1 : 1 ratio (1 μg of total plasmid) for co-transfection. Those plasmids were replaced with the empty vectors, when they were not used. Data are presented as the means ± S.E. from 4 experiments conducted in a single determination. *P < 0.05 compared with the value for mock cells; †P < 0.05 compared with the value for the cells expressing ENBT1 alone. Statistical significance was assessed by ANOVA followed by Dunnett's test.

Fig. 5. Effect of stable expression of GFP-ENBT1 and/or HSV-TK on GCV uptake in MDCKII cells. The uptake of [^{3}H]GCV (30 μM) was evaluated for 5 min (A) and 60 min (B) at 37°C and pH 7.4. Data are presented as the means ± S.E. from 4 experiments conducted in a single determination. *P < 0.05 compared with the value for mock cells; †P < 0.05 compared with the value for the cells expressing GFP-ENBT1 alone. Statistical significance was assessed by ANOVA followed by Dunnett's test.

Fig. 6. Effect of stable expression of GFP-ENBT1 and/or HSV-TK on GCV-induced cytotoxicity in MDCKII cells. The cells were incubated for 72 h in DMEM in the presence of GCV at varied concentrations, or in its absence, and their viability was determined by the WST-8 assay and normalized to that observed in the absence of GCV. Data are presented as the means ± S.E. from 4 experiments conducted in a single determination. *$P < 0.05$ compared with the value for mock cells at each GCV concentration; †$P < 0.05$ compared with the value in the absence of GCV in the indicated cell type. Statistical significance was assessed by ANOVA followed by Dunnett's test.

Fig. 7. Kinetic analysis of the uptake of GCV by GFP-ENBT1 stably expressed with HSV-TK in MDCKII cells. (A) Time course of the uptake of [^{3}H]GCV (30 μM) at 37°C and pH 7.4. Data are presented as the means ± S.E. from 4 experiments conducted in a single determination. (B) Concentration dependence of the specific uptake rate of [^{3}H]GCV for 30 min at 37°C and pH 7.4 in cells expressing GFP-ENBT1 with HSV-TK. The specific uptake rate was estimated by subtracting the uptake rate in mock cells from that in cells expressing ENBT1. Data are presented as the means ± S.E. from 3 experiments conducted in duplicate. The K_m and V_{max} are 96.7 ± 18.4 μM and 51.8 ± 5.8 pmol/min/mg protein, respectively, as the means ± S.E. from 3 experimental profiles of the uptake rate *versus* concentration..

Fig. 8. Western blot analysis of the protein expression of endogenous ENBT1 and transiently expressed FLAG-HSV-TK in various cancer cell lines. The analysis was performed using the whole cell lysate samples (30 μg aliquots). ENBT1 was detected as the band corresponding to its predicted molecular mass of about 55 kDa. The blots of β-actin are shown for reference.

Fig. 9. Effect of transient introduction of FLAG-HSV-TK on GCV uptake in various cancer cell lines. The uptake of [^{3}H]GCV (30 μM) was evaluated for 5 min at 37°C and pH 7.4. Panels A and B are for ENBT1-rich cell lines and ENBT1-poor ones, respectively. Data are presented as the means ± S.E. from 4 experiments conducted in a single determination. *P < 0.05 compared with the value for mock cells, as assessed by Student's *t* test.

Fig. 10. Effect of transient introduction of FLAG-HSV-TK on GCV-induced cytotoxicity in various cancer cell lines. Cells were incubated for 68 h in a growth medium (RPMI 1640 for HCT-15 cells and DMEM for the other cells) in the presence of GCV (30 μM), or in its absence, and their viability was determined by the WST-8 assay and normalized to that observed in the absence of GCV. Data are presented as the means ± S.E. from 4 experiments conducted in a single determination. *P < 0.05 compared with the value for mock cells, as assessed by Student's *t* test.

Fig. 11. Effect of silencing of ENBT1 on GCV uptake and GCV-induced cytotoxicity in HeLa cells transiently expressing FLAG-HSV-TK. Experiments were conducted in cells treated for transient expression of FLAG-HSV-TK and in mock cells, with or without simultaneous silencing of ENBT1 using its specific siRNA. (A) The protein expression levels of endogenous ENBT1 and transiently expressed FLAG-HSV-TK in HeLa cells were analyzed by western blotting. The blots of β-actin are shown for reference. (B) The uptake of [^{3}H]GCV (30 μM) was evaluated for 5 min at 37°C and pH 7.4. (C) Cells were incubated for 72 h in DMEM in the presence of GCV (30 μM), or in its absence, and their viability was determined by the WST-8 assay and normalized to that observed in the absence of GCV. Data are presented as the means ± S.E. from 4 experiments conducted in a single determination in

JPET Fast Forward. Published on November 2, 2016 as DOI: 10.1124/jpet.116.236984
This article has not been copyedited and formatted. The final version may differ from this version.

panels B and C. *$P < 0.05$ compared with the value for the cells expressing FLAG-HSV-TK and treated with control siRNA, as assessed by ANOVA followed by Dunnett's test.

JPET Fast Forward. Published on November 2, 2016 as DOI: 10.1124/jpet.116.236984
This article has not been copyedited and formatted. The final version may differ from this version.

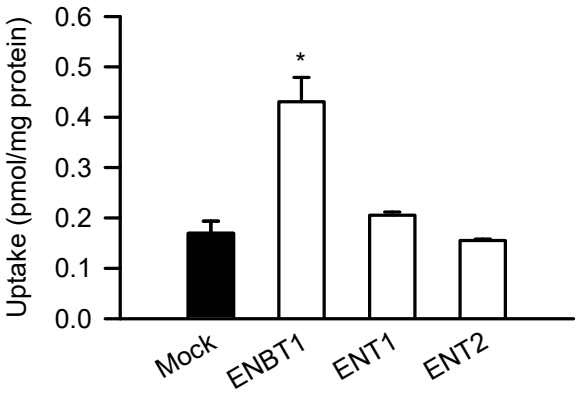

Fig. 1

JPET Fast Forward. Published on November 2, 2016 as DOI: 10.1124/jpet.116.236984
This article has not been copyedited and formatted. The final version may differ from this version.

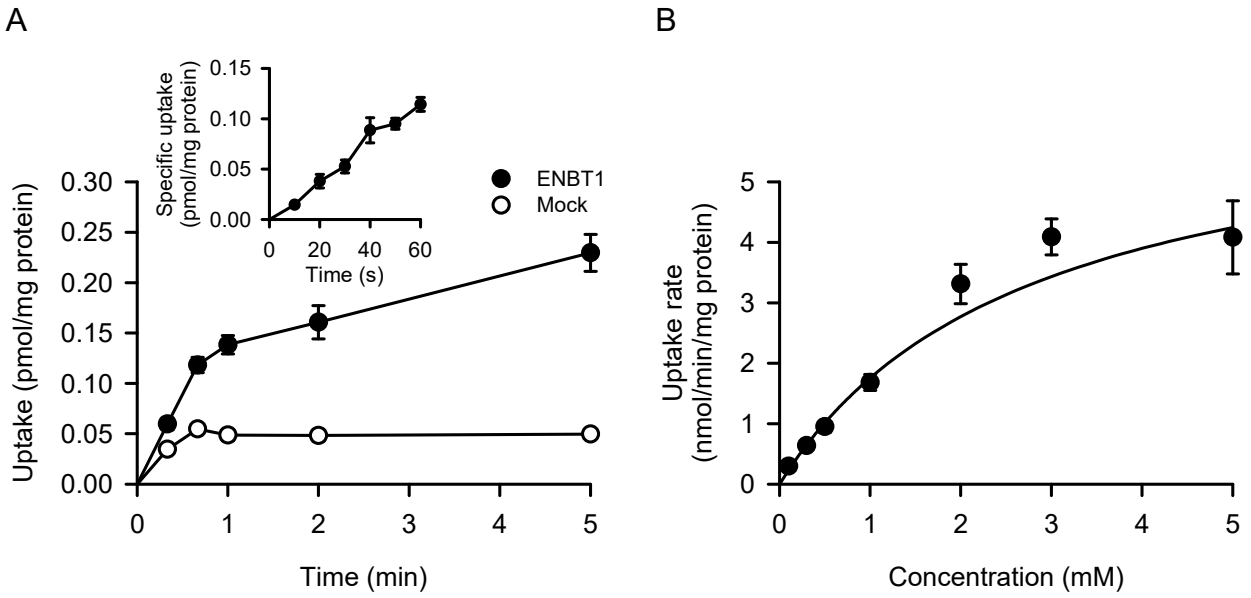

Fig. 2

JPET Fast Forward. Published on November 2, 2016 as DOI: 10.1124/jpet.116.236984
This article has not been copyedited and formatted. The final version may differ from this version.

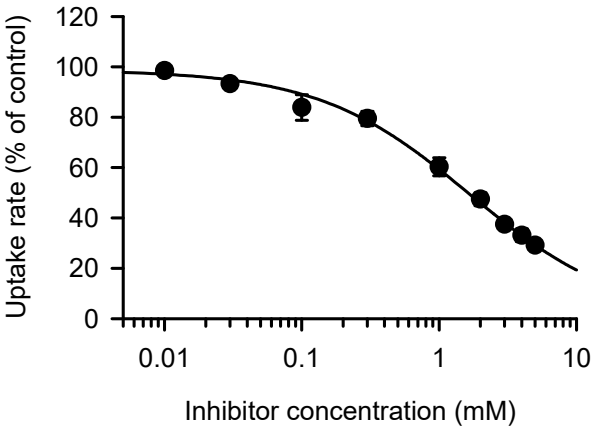

Fig. 3

JPET Fast Forward. Published on November 2, 2016 as DOI: 10.1124/jpet.116.236984
This article has not been copyedited and formatted. The final version may differ from this version.

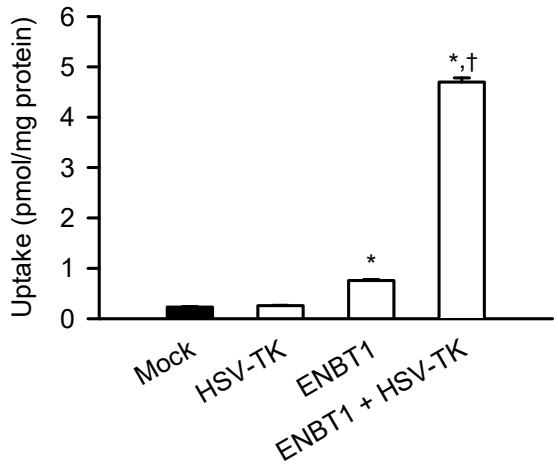

Fig. 4

JPET Fast Forward. Published on November 2, 2016 as DOI: 10.1124/jpet.116.236984
This article has not been copyedited and formatted. The final version may differ from this version.

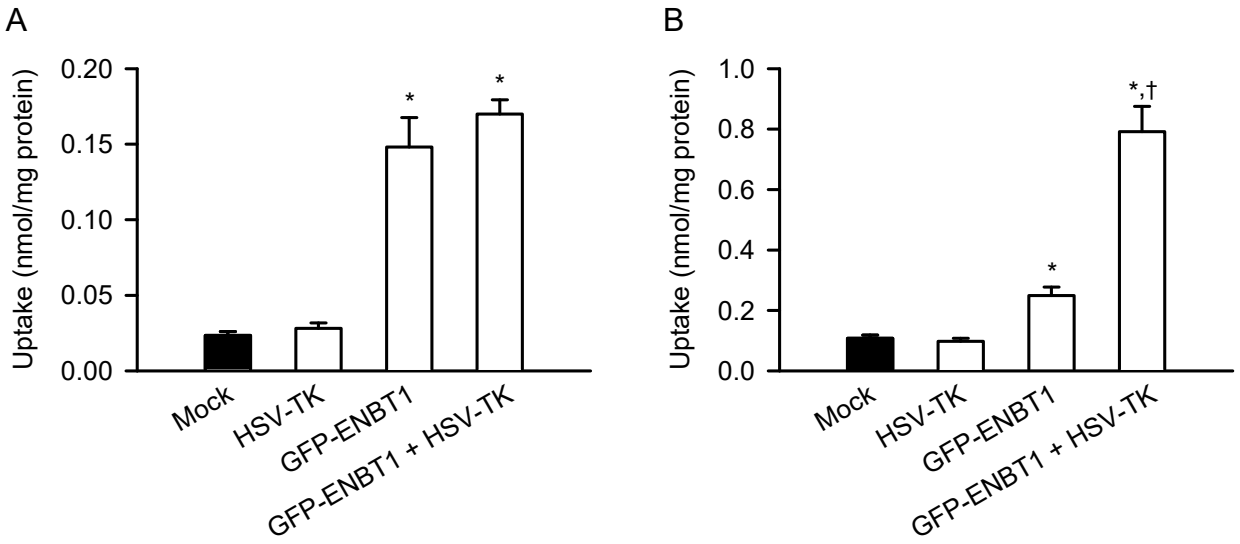

Fig. 5

JPET Fast Forward. Published on November 2, 2016 as DOI: 10.1124/jpet.116.236984
This article has not been copyedited and formatted. The final version may differ from this version.

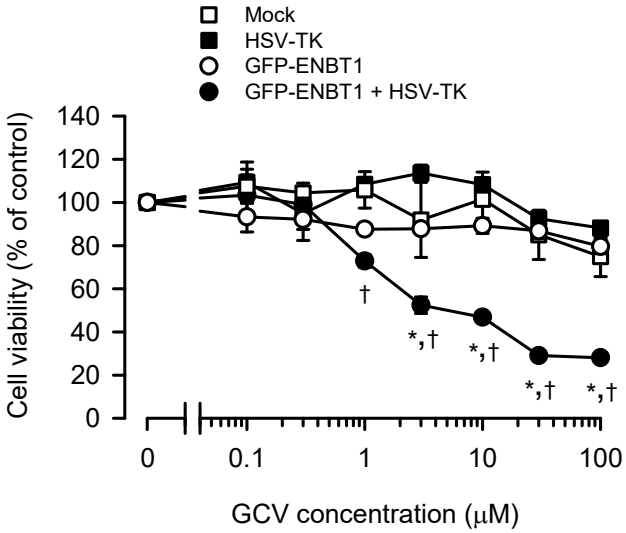

Fig. 6

JPET Fast Forward. Published on November 2, 2016 as DOI: 10.1124/jpet.116.236984
This article has not been copyedited and formatted. The final version may differ from this version.

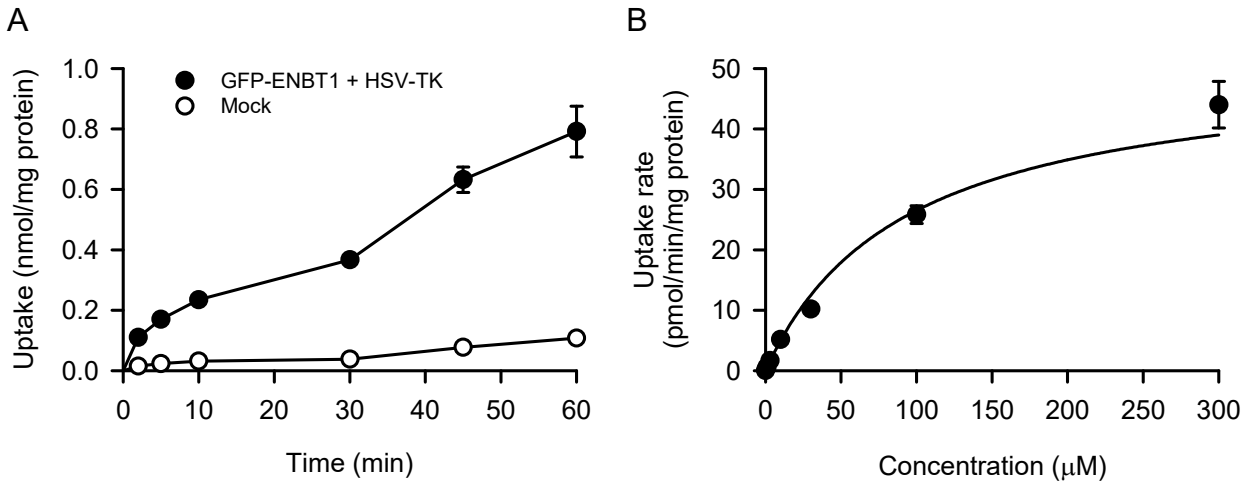

Fig. 7

JPET Fast Forward. Published on November 2, 2016 as DOI: 10.1124/jpet.116.236984
This article has not been copyedited and formatted. The final version may differ from this version.

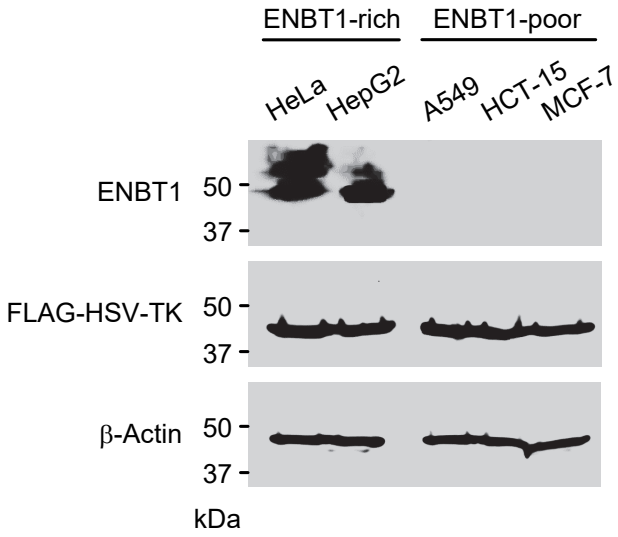

Fig. 8

JPET Fast Forward. Published on November 2, 2016 as DOI: 10.1124/jpet.116.236984
This article has not been copyedited and formatted. The final version may differ from this version.

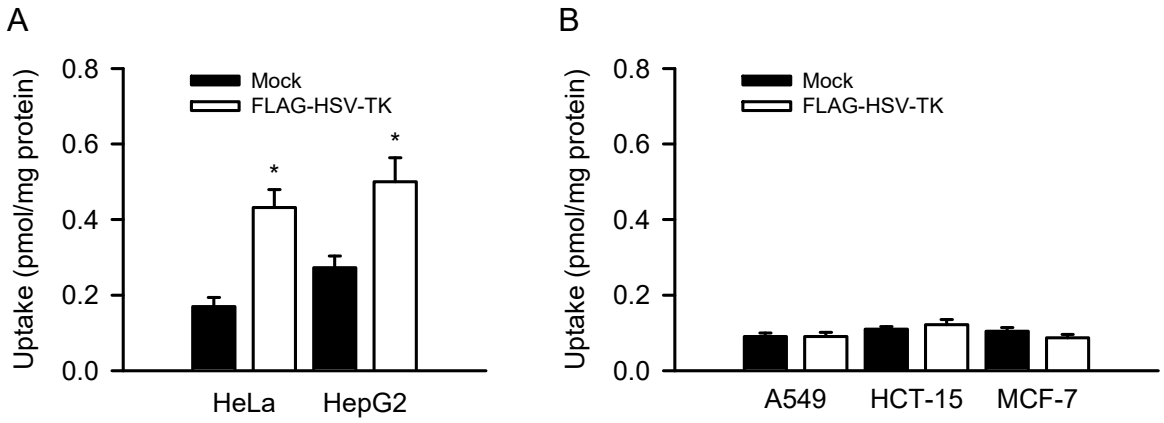

Fig. 9

JPET Fast Forward. Published on November 2, 2016 as DOI: 10.1124/jpet.116.236984
This article has not been copyedited and formatted. The final version may differ from this version.

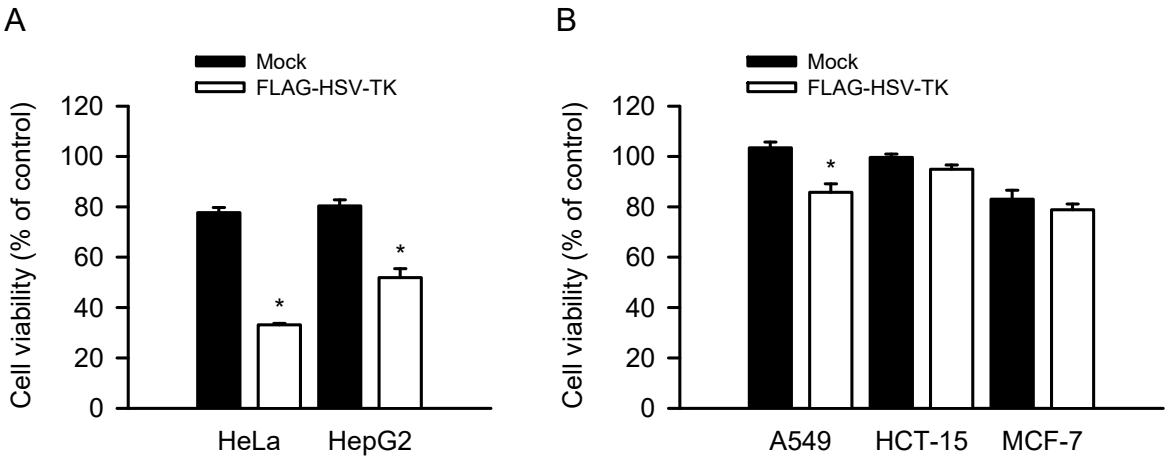

Fig. 10

JPET Fast Forward. Published on November 2, 2016 as DOI: 10.1124/jpet.116.236984
This article has not been copyedited and formatted. The final version may differ from this version.

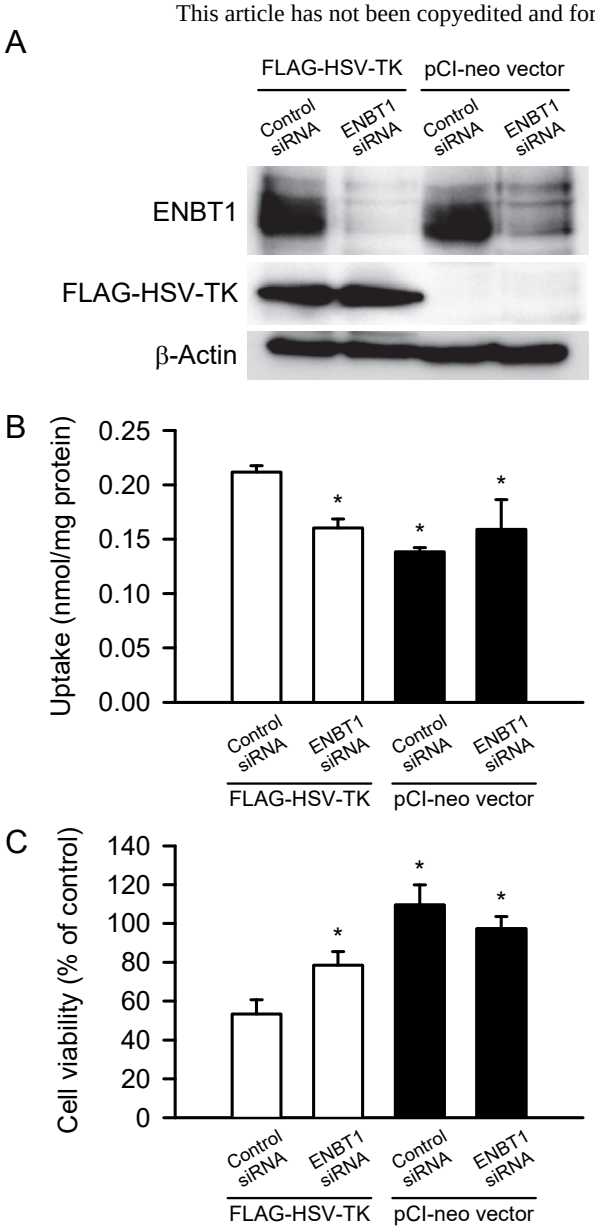

Fig. 11